18th International Conference on Protection & Automation in Power System
Shahrood University of Technology
January 9, 2024 - January 10, 2024

A Novel Current Based Protection Scheme for Internal/External Fault Detection in Islanded Two Interconnected AC Microgrid

Saber Armaghani
Postdoc Researcher
Electrical & Computer Engineering Faculty
Semnan University
Semnan, Iran
s.armaghany@semnan.ac.ir

Zahra Moravej
Electrical & Computer Engineering Faculty
Semnan University
Semnan, Iran
zmoravej@semnan.ac.ir

***Abstract*— This paper proposes a novel current-based protection scheme for detecting and distinguishing internal from external faults in Interconnected AC Microgrids (IAC-MGs). The proposed protection scheme uses the time domain-based dq0 transformation due to the fault current level being low in islanded IAC-MGs, and a low sensitivity protection scheme to the fault current level is necessary for the protection of MG and IAC-MG. Numerical results in the two IAC-MG test case shows that the proposed protection scheme can detect and distinguish between internal and external faults. Also, the proposed protection scheme has low sensitivity to the fault current level and does not require the communication system for fault detection.**

Keywords-Current based protection, interconnected AC Microgrids, dq0 transformation, internal/external fault detection

I. Introduction

In recent years, Distributed Generations (DGs) such as Wind Turbines (WT) and Photovoltaic cells (PV) at medium or low voltage levels have integrated efficiently as a subsystem named Microgrid (MG) and supplied electric energy for local load demands [1]. Micrograms (MGs) can operate in grid-connected, islanded, and Interconnected modes. Interconnected Microgrids (IMGs) refer to a group of MGs with geometrically DC or AC connection nodes [2]. AC MGs connect each other by either DC back-to-back converters [3] or AC tie lines or Circuit Berker (CB) [2]. Usually, when the distance between microgrids is large, alternating microgrids are connected to each other with a tie line. Moreover, IMGs can be operated in grid-connected or island mode. IMGs are more flexible, reliable, and resilient than single MGs [2] in island mod. However, AC IMGs with tile line connection increase the protection challenges spatially in the fault detection context because they must be reliable in both single MGs and the set of interconnected MGs according to topologies [2]. In other words, protection schemes must satisfy both single MGs and IMGs challenges.

The main challenge in single MGs consists of variable fault current levels by changing the operation modes of MGs. An adaptive protection scheme [4] is proposed to deal with variating fault current levels by adjusting a group setting mechanism for overcurrent protection. However, adaptive protection approaches usually impose the overall cost of protection since they require advanced communication and monitoring systems. Differential protection approaches are another scheme proposed for MG protection by the fast, selective, and low-sensitive characteristics [5]. However, differential protection approaches require synchronous measures from different locations of MG and high-bandwidth communication systems. Artificial intelligence (AI)-based advanced signal processing approaches are proposed to identify and distinguish the fault [6]. However, the large number of realistic training data sets is the main drawback of AI-based protection schemes for single MGs. The active protection scheme is another single MG protection that identifies the fault by measuring the control signals of DG [7]. Although active protection schemes provide significant solutions in a fault detection context at single MGs with low sensitivity to fault current levels, these schemes are very complex and hard to implement in the real environment. These schemes are complicated since matching DG's controlling systems to protection issues requires modifications for control algorithms and design. The traveling wave protection scheme is proposed in [8] for fault detection in a low sensitivity to fault current level. However, the network of MG usually consists of short-distance transmission lines that cause the sampling frequency to increase in the traveling wave protection scheme. The energy-based transient wavelet protection scheme is proposed in [9] for fault detection in MGs in low sensitivity to current fault level manner. However, a low-cost communication

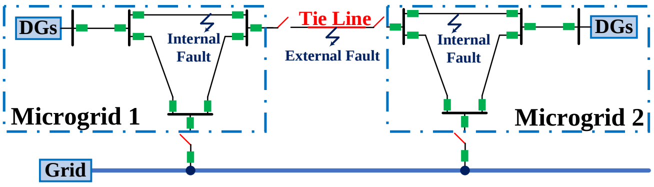

Figure 1. Typical two IMGs

system is still needed to develop a protection system, which can cause security challenges for the single MGs.

Thus, the mentioned protection schemes cannot efficiently detect the fault conditions in IAC-MG. In addition to the mentioned problems about single MGs, distinguishing between internal and external faults is the other challenge in IMGs. Internal fault refers to fault occurrences in MGs. However, the external fault refers to fault occurrences in the connection system, which links every MG in the IMG network. A directional overcurrent protection scheme is proposed in [10] to detect internal faults only and cannot detect external faults in IMGs. Also, measured voltage and current are needed in [10] to construct the proposed directional overcurrent scheme. Also, the proposed protection scheme in [10] is a high-cost communication protection scheme.

A protection scheme based on dq0 transformation is proposed in this paper to detect and distinguish internal from external faults in IAC-MG. The proposed protection scheme can quickly detect both three-phase, asymmetrical faults and high-impedance faults without requiring the communication system. Moreover, it does not operate in heavy load pickup by suitable adjusting the load pickup value and protection threshold. Also, the proposed protection scheme uses the current only in protection zone.

The rest of this paper is organized as follows: IAC-MG is described in section II. The proposed protection scheme is presented in section III. Numerical results are provided in section IV to illustrate the efficiency and selectivity of the proposed protection scheme. Finally, the conclusion is drawn in section v.

II. Protection perspective for IAC-MG

A brife description on IAC-MG in protection perspective is presented in this section.

A. IAC-MG definition

An Interconnected microgrid is defined as more than one electrically coupled microgrid in this group that is controlled and operated in a coordinated fashion. These groups can enhance stability, power quality, and reliability as several MGs are connected. Usually, IMGs allow interconnection in normal conditions and require disconnection from the distribution system under emergency (fault) conditions. Therefore, these groups can reserve and share energy in critical conditions and minimize emergency load-shedding requirements. However, protection issues are more difficult than the mentioned advantages in IMGs.

B. Two interconnected AC microgrid topology

Fig.1 shows a typical two islanded IMGs. Two interconnected AC microgrid is one of the IMG topologies called two single MG connected by a single feeder. According to Fig. 1, each MG can connect to each other and to the distribution system. Also, MGs can be connected to each other through switches, tie-lines and transformers, and DC back-to-back converters. According to Fig. 1, each MG can connect to each other and to the distribution system.

C. Protection isuess in Typical two IMGs

The most critical issue in the island IMGs with DG resources is the low fault current level that can cause false tripping problems. For example, some of the equipment of a single MG might be disconnected when the fault occurs in the tie-line, or the tie-line can be disconnected when the fault has occurred in one of the single MG. Thus, traditional protection schemes such as distance relays fail in the IMGs. Also, low and variable fault current levels are required for a low sensitive protection scheme. Moreover, response time of protection is the other challenges in single and interconnected MGs. Thus, the fault detection scheme in two IMGs must overcome challenges such as low and variable fault current levels, distinguishing between internal and external faults, and fast response. The proposed protection scheme provides results with suitable low sensitivity to fault current level, distinguishing internal/external faults, and fast response characteristics. The proposed protection scheme is presented in the next section.

III. Proposed Detection and Distinguishing protection scheme

The proposed protection scheme uses the measured current signal only. The flowchart of the proposed protection scheme is shown in Fig. 2. According to Fig. 2, the proposed protection scheme includes five main steps as follows:

step 1) measuring k^{th} sample of MG three-phase current

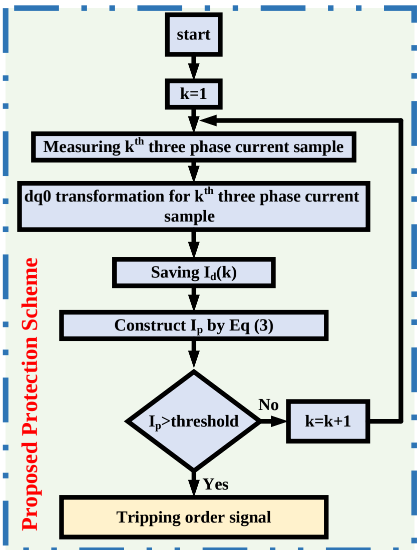

Figure 2. Flowchart of the proposed current based protection scheme

step 2) transforming from “abc” current to “dq0” for k[th] current sampled,

step 3) saving k[th] transformed current in “d” axis,

step 4) calculating Identification Index named I_p (which will be presented in section III-B),

step 5) comparing I_p with the pre-defined threshold. If I_p is bigger than the threshold, then send a trip signal to the circuit breaker and go to step 6. Otherwise, measure the next sample (k=k+1) three-phase current and go to step 2,

Step 6) stop.

A. Park Transformation dq0

In this paper, park transformation, which is proposed in [11, 12] as a low-sensitive method for fault detection problems, is used for transforming system “abc” to “dq0” frame to simple and low-sensitive detection of current and internal/external classification. Then, the proposed current-based protection method is constructed to detect and classifies internal/external fault in two IAC-MG. The dq0 frame analyzes the current behavior of two IAC-MG to recognize useful patterns in internal/external fault detection. Then, by applying dq0, fault can be detect using Identification Index (I_p), which is presented in the next section. The dq0 component transformation is written as follows:

$$\left[i_{dq0}\right]=\left[T_{dq0}\right].\left[i_{abc}\right] \tag{1}$$

where the i_{dq0} is the dq0 component of current, the T_{dq0} is the transformation matrix, and the i_{abc} is the system “abc” current. The T_{dq0} is presented by equation (2) as follows:

$$\left[T_{dq0}\right]=\sqrt{\frac{2}{3}}\begin{bmatrix}\cos\theta & \cos\left(\theta-2\pi/3\right) & \cos\left(\theta+2\pi/3\right)\\ -\sin\theta & -\sin\left(\theta-2\pi/3\right) & -\sin\left(\theta+2\pi/3\right)\\ \sqrt{2}/2 & \sqrt{2}/2 & \sqrt{2}/2\end{bmatrix} \tag{2}$$

B. Identification Index

After calculating “dq0” component of kth system “abc” samples, the Identification Index (I_p) is written as follows:

$$\begin{aligned}I_p&=\sqrt{\left(I_{sd}\right)^2+\left(I_{sd}\right)^2+\left(I_{s0}\right)^2}\\ I_{sd}&=i_d\left(k\right)-i_d\left(k-1\right)\\ I_{sd}&=i_q\left(k\right)-i_q\left(k-1\right)\\ I_{s0}&=i_0\left(k\right)-i_0\left(k-1\right)\end{aligned} \tag{3}$$

where the I_p is the proposed identification index, i_d, i_q, and i_0 is current in dq0 frame for k[th] and (k-1)[th] sample, respectively. In fact, I_p is Euclidean distance of difference between dq0 samples.

IV. Numerical Results

In this section, the proposed current based protection scheme is implemented in a two-IAC-MG in island mode. Two IAC-MG is modeled in $EMTP_{RV}$ software. Island mode operation of the IAC-MG is the worst case in the fault detection context since the fault current level is low in this operation mode.

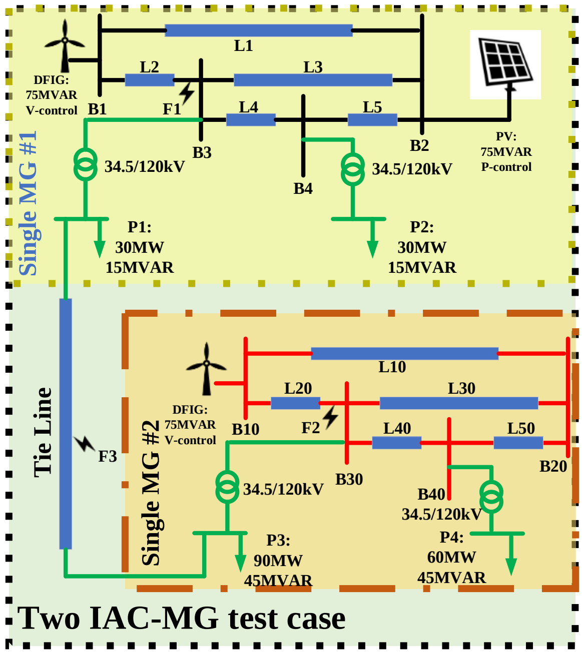

Figure 3. Two IAC-MG test case

TABLE I. MG’S AND TIE LINE’S PARAMETERS

Line	Electrical Parameters						Length (km)
	R^+ (Ω/km)	L^+ (mH/km)	C^+ (µF/km)	R^0 (Ω/km)	L^0 (mH/km)	C^0 (µF/km)	
L1	0.3	3	0.008	0.02	0.9	0.0126	100
L2	0.3	3	0.008	0.02	0.9	0.0126	50
L3	0.3	3	0.008	0.02	0.9	0.0126	75
L4	0.3	3	0.008	0.02	0.9	0.0126	50
L5	0.3	3	0.008	0.02	0.9	0.0126	50
Tie Line	0.3	3	0.008	0.02	0.9	0.0126	100

A. Two IAC-MG system description

The single-line diagram of the 120 kV, 50 Hz two IAC-MG test system in island mode, which consists of two same single MG, is shown in Fig. 3. Line and tie line parameters for MG #1 are presented in Table .1. The line parameters of MG #2 are the same as line parameters of MG#1 as mentioned in Table. 1. Distributed energy resources (DERs) used in the test case are operated in V- and P-control mode for WT and PV, respectively. The rated power of DERs is 75MVA. Voltage-control mode is a secondary concept to WT’s reactive control, which is formed by a proportional voltage control in the outer control loop of WTs. The schematic diagram of V-mode control is shown in Fig. 4. Voltage control follows the voltage references sent by DFIG at the point of grid interconnection. A detailed description of how to design the WT controller is presented in [13]. Also, the P-control mode is considered for PV in this paper to work in MG. Since P-Q control is a common control mechanism for PV in islanded MG [14]. Two feedback control loops are commonly used to develop a P-Q control scheme for PV in islanded MG,

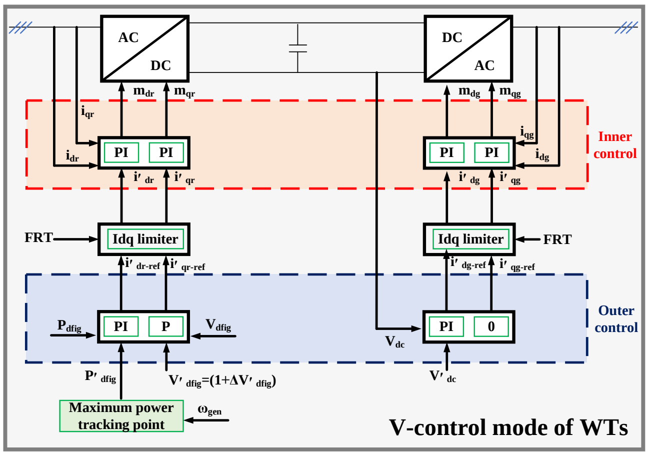

Figure 4. Schematic diagram of V-control mode for WT

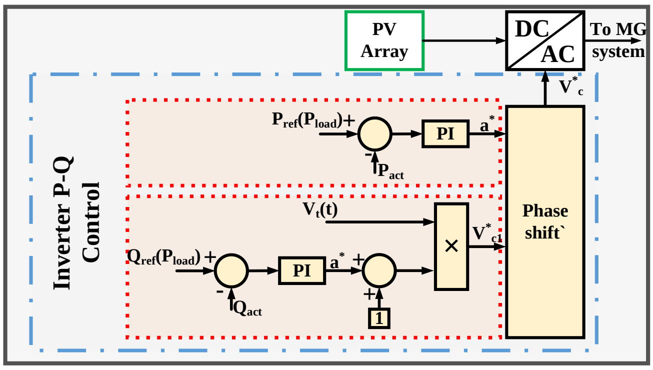

Figure 5. Schematic diagram on P-control mode for PV

TABLE II. DERS' PARAMETERS

DER	Rated Power		Converter control			
	S (MVA)	*V* (kV)	k_v	*Sample rate* (Hz)	*PWM* (Hz)	V_{dc}*-control* (ms)
WT	75	34.5	2	12500	2500	-
PV	75	34.5	2	22500	4500	100

TABLE III. DERS' PARAMETERS

MG	Rated Power			
	load	*P* (MW)	*Q* (MVAR)	*V* (kV)
#1	1	30	15	120
	2	30	15	120
#2	1	90	45	120
	2	60	45	120

according to Fig. 5. A detailed description about how to design the P-Q controller for PV is presented in [14]. Parameters of WT and PV are presented in Table. II.

Parameters of load in both single MGs are presented in Table. III. According to Table. II and Table. III, the apparent power flowed from single MG #1 to single MG #2.

B. *Three phase fault detection*

Three LLL fault occurrence scenarios are provided in this section at F1, F2, and F3 locations. The fault is assumed to have occurred at 10ms in each provided scenario. Three phases, dq0, and I_p currents for the fault scenario in F1 are shown in Fig. 6. It is necessary to mention that Fig. 6 shows the results measured only in single MG #1. According to Fig. 6 a, the magnitude of three phase currents is increased after 10 msec due to fault occurrence. Also, the I_d and I_q are changed after fault occurrence at 10 msec. Thus, the proposed I_p-based on dq0 transformation analysis can detect fault F1, which is an internal fault. It can clearly be seen from Fig. 6 c that the magnitude of I_p is suddenly increased from 0 to approximately 80 A after just one sample after fault occurrence at 10 msec. The proposed I_p for L20 in single MG #2 and tie line is shown in Fig. 7a and Fig. 7 b, respectively. It can be seen from Fig. 7 that the maximum value of I_p at both L20 and tie-line is less than 0.5, which illustrates the ability of the proposed protection scheme to detect and distinguish the internal fault from the external or internal fault at the other single MG. Similarly, it assumed that a LLL fault is occurred in F2 location at 10 msec. The measured three-phase, dq0 sequence current and I_p are shown in Fig. 8 for fault occurrences at F2 in MG #2. According to Fig. 8, it can be seen that the dq0 sequence current is variated after fault occurrence at 10 msec. Also, I_p is suddenly changed from 0 to 75 in just 1

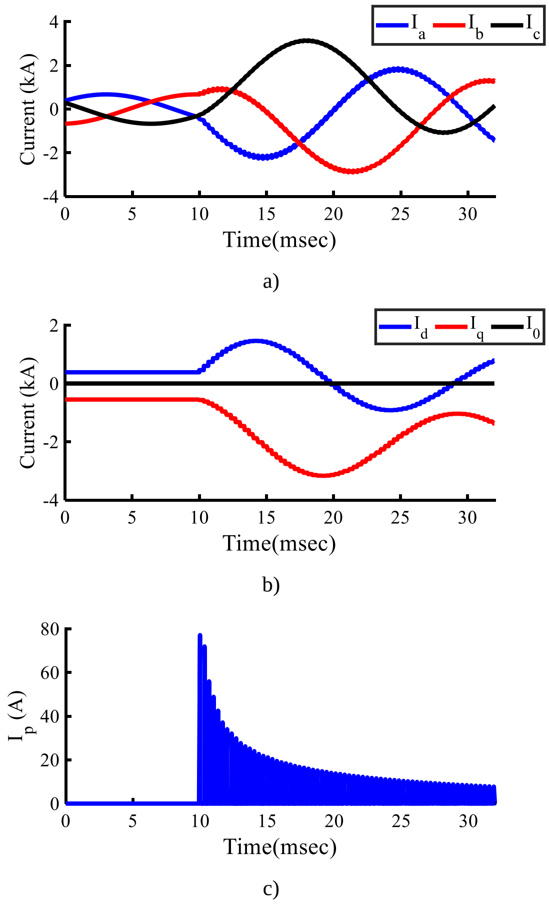

Figure 6. Result on MG #1 associated LLL fault occurances in F1, a) three phase current, b) dq0 cecuance current, c)the proposed I_p

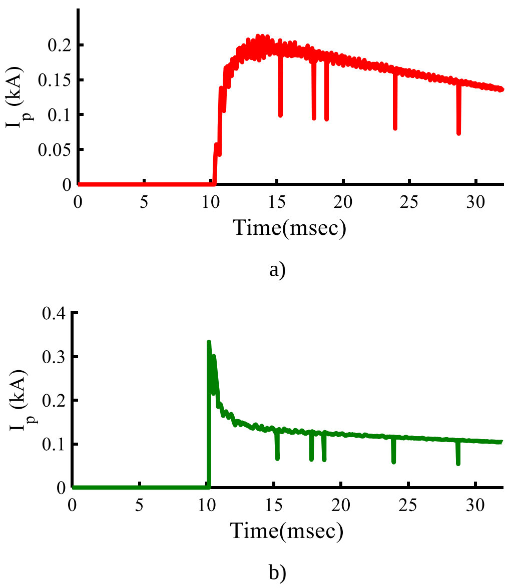

Figure 7. The proposed I_p for measured data from MG #2 and tie line in fault occurrence scenario at F1, a) L20, b) tie line in half distance of total line length

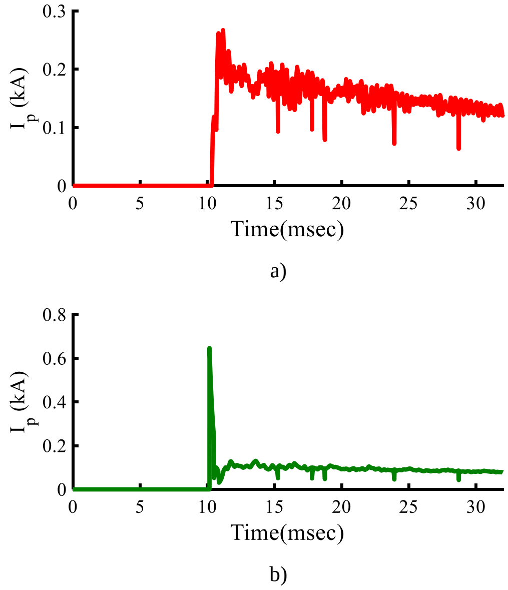

Figure 9. The proposed I_p for measured data from MG #1 and tie line in fault occurrence scenario at F2, a) L2, b) tie line in half distance of total line length

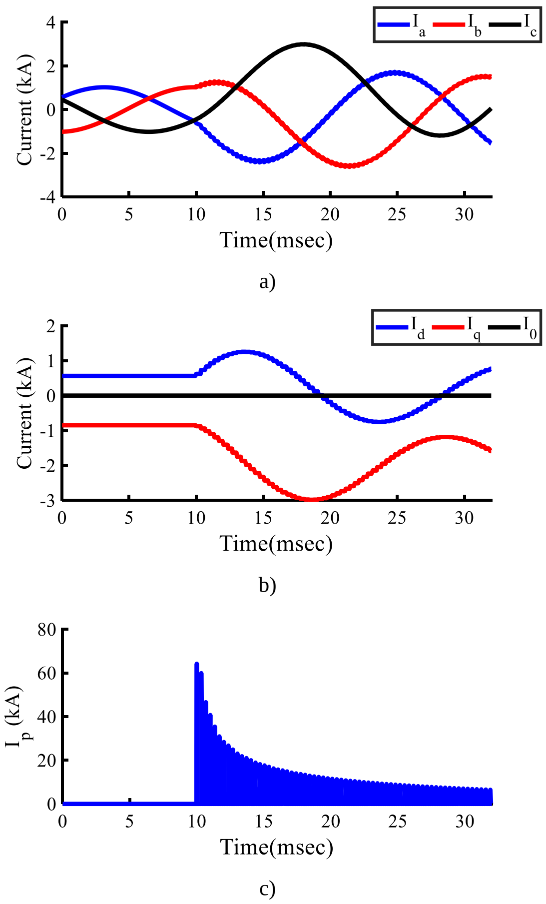

Figure 8. Result on MG #2 associated LLL fault occurances in F2, a) three phase current, b) dq0 cecuance current, c)the proposed I_p

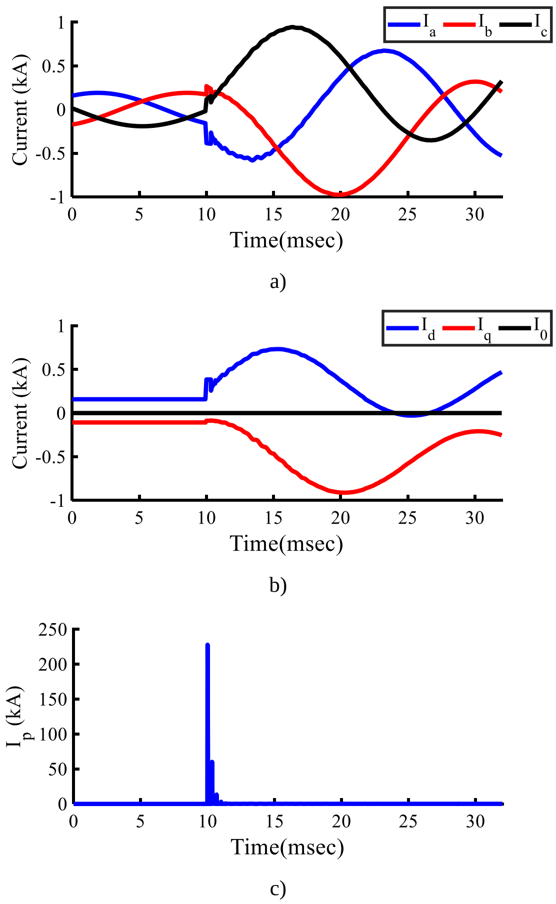

Figure 10. Result on tie line associated LLL fault occurrences in F3, a) three phase current, b) dq0 sequence current, c)the proposed I_p

sample after fault occurrence at F2 in the L20 measurement current point of view. Also, I_p from L2 and tie line point of view when fault F2 has occurred in MG #2 are shown in Fig. 9. According to Fig. 9, it can be seen that I_p is less than 0.8 for both L2 and tie line relays. That means that only the relay on L20 can detect fault F2. Finally, it assumed that fault F3 occurred at half distance in the tie line at 10 msec. The measured three phase current, dq0 sequences current, and obtained I_p are shown in Fig. 10. It can be seen from Fig. 10a that three phase currents are distorted after fault occurrence at 10 msec. Also, dq0 sequence current amounts are constant before fault F3 at 10 msec, but their amounts are changed after fault F3 at 10 msec. The value of I_p is zero before fault occurrence at 10 msec, but its value is approximately 250 A just 1 sample after fault F3 occurrence at 10 msec. The Identification Index (I_p) for L2 and L20 in fault scenario F3 is shown in Fig. 11. According to Fig. 11, the I_p value is less than 0.8 for L2 and L20. Then, external fault F3 can be detect only from the installed relay on the tie-line.

A conclusion about this section is presented in Table. V. According to Table. V, the I_p value of MG #1 is the highest in the F1 fault scenario, which occurred in L2, but the I_p value is very few for MG #2 and tie-line. Thus, only the relay on L2 detects fault as an internal fault. Similarly, in fault scenario F2, the I_p value in MG #2 is the highest and more than 75, which can easily be detected as an internal fault just by the installed relay on L20. Finally, the external fault F3, according to Table.

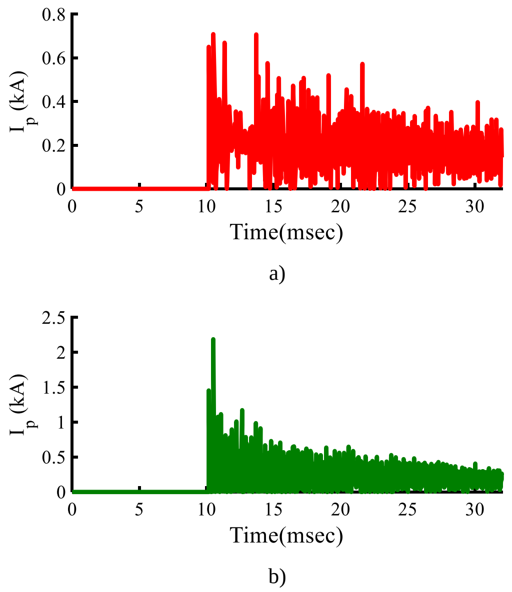

Figure 11. The proposed Ip for measured data from MG #1 and MG #2 in fault occurrence scenario at F3, a) L2, b) L20

TABLE IV. LLL FAULT DETECTION BY IDENTIFICATION INDEX

Fault scenario	I_p			Threshold
	MG#1	*MG#2*	*Tie line*	
F1	80	0.05	0.4	5
F2	0.12	70	0.75	5
F3	0.7	1.5	240	35

IV can be detected only by the installed relay on the tie-line since the value of I_p is highest for the tie-line. The value of I_p is 0.7 and 1.5 for MG #1 and MG #2, respectively. Thus, the proposed protection scheme can successfully detect and classify the internal/external faults in two IAC-MG. Also, the detection process is carried out in just 1 sample after fault occurrence for all fault F1, F2, and F3 scenarios. Thus, the proposed protection is fast enough to be used in two IAC-MG.

C. *Asymmetrical fault detection*

In this section, asymmetrical faults such as LL, LLG, and LG for fault scenarios in F1, F2, and F3 locations are provided in the two IAC-MG test cases to investigate the ability of the proposed protection scheme in asymmetrical fault detection. The asymmetrical fault, with the mentioned occurrence characteristic in the previous section, is similarly considered in this section. The fault resistance is assumed to be zero in this section. The I_p value for all the mentioned fault scenarios is presented in Table. V for MG #1, MG #2, and the tie-line. According to Table. V, the I_p value is the highest for LLG, LL, and LG fault occurrence in MG #1 as the F1 fault scenario in this table. Also, fault scenario F2 provides the highest I_p value for LLG, LL, and LG in MG#2, that distinguishes the internal fault in MG#2 from the external fault in the tie-line and the internal fault in MG #1. Moreover, the ability of the proposed protection scheme to detect and distinguish external fault in the tie-line from internal fault in both MG #1 and MG #2 is illustrated by the presented results of the I_p value in Table. V. The I_p value is the highest in fault scenario F3 for LLG, LL, and LG, which presents the asymmetrical fault in the tie-line to be detected by the proposed protection scheme.

D. *High impedance fault detection*

In this section, LG fault with 400Ω fault resistance value is considered to illustrate the ability of the proposed protection scheme in high impedance fault detection. Also, three fault scenarios, such as F1, F2, and F3, are considered in this section, and the obtained results of I_p value are present in Table. VI. According to Table. VI, the proposed protection scheme can detect high impedance fault since the highest I_p value in each fault scenario F1, F2, and F3 is more than thresholds. Moreover, distinguishing internal from external faults in a two- IAC-MG is

TABLE V. ASYMMETRICAL FAULT DETECTION BY THE PROPOSED SCHEME

Fault type	Fault scenario	I_p			Threshold
		MG#1	*MG#2*	*Tie line*	
LLG	F1	74.5	0.055	0.32	5
	F2	0.12	64	0.64	5
	F3	0.54	1.2	190	35
LL	F1	74	0.055	0.32	5
	F2	0.11	63.9	0.64	5
	F3	0.53	1.18	186.32	35
LG	F1	39	0.021	0.15	5
	F2	0.02	30.2	0.27	5
	F3	0.30	0.67	118.2	35

TABLE VI. HIGH IMPEDANCE FAULT DETECTION BY THE PROPOSED SCHEME

Fault scenario	I_p			Threshold
	MG#1	*MG#2*	*Tie line*	
F1	9.42	0.005	0.04	5
F2	0.004	7.3	0.065	5
F3	0.01	0.22	38.2	35

TABLE VII. HIGH LOAD PICKUP

scenario	Pickup value		I_p			Threshold		
	MW	*MVA*	*MG#1*	*MG#2*	*Tie line*	*MG#1*	*MG#2*	*Tie line*
P1	18	9	0.2	0.5	33.22	5	5	35
P3	30	15	0.8	1.7	31.45			

TABLE VIII. LLL FAULT DETECTION IN GRID-CONNECTION MODE BY THE PROPOSED SCHEME

Fault scenario	I_p			Threshold
	MG#1	*MG#2*	*Tie line*	
F1	118.63	0.83	5.12	25
F2	1.95	118.59	10.22	25
F3	12.42	22.54	498.2	35

guaranteed by the proposed protection scheme in a high-impedance fault detection context. This guarantee is achieved by the high difference between the I_p value of the other protection zone and the pre-defined threshold for each MG and tie-line. It is necessary to mention that the presented thresholds in Table VI, which is adjusted by providing all considered fault scenarios at island IAC-MG in this paper, are suitable for 400Ω LG fault detection (High impedance scenario).

E. High load pickup

In this section, two load pickup scenarios are considered to illustrate the no detectability property of the proposed protection scheme. It is assumed in this section that both load P1 and P3 are separately picked up at 10 msec as mentioned in Table. VII. The results of the pickup simulation are presented in Table VII. It can be understood from Table. VII that the highest I_p values are less than the threshold.

F. LLL fault in grid-connected mode

In this section, the grid-connected mode effect on the fault detection property of the proposed protection scheme is investigated by considering the 63 kV source-connected situation at the middle of the AC tie line. Then, LLL fault occurrence scenarios at F1, F2, and F3 separately are simulated to investigate the performance of the proposed protection scheme in internal/external fault detection tasks. The numerical results are presented in Table VIII. It can be seen from Table VIII that the proposed scheme can detect internal/external faults in grid-connected mode operation of IAC-MG by readjusting thresholds.

V. Conclusions

By increasing DERs penetration in single MGs and interconnected MGs, protection converts into a challenging issue in both single MGs and interconnected MGs. Protection speed, fault current level sensitivity, low-cost communication, and internal/external distinguishment are the main challenges in single MG and IAC-MG. A time domain signal-processing-based protection scheme was proposed in this paper to overcome these protection challenges in the two IAC-MG. The proposed protection scheme used dq0 sequence transformation and the proposed identification index to detect and distinguish between internal and external faults in two IAC-MG. Numerical results in a two-IAC-MG test case with specific operation condition illustrated the detectability property of the proposed protection scheme in fault detection. Adjusting optimum threshold and uncertainty operation condition are not in the scope of this paper and will be considered in future work.

REFERENCES

[1] D. Liu, A. Dyśko, Q. Hong, D. Tzelepis, and CD. Booth, “Transient wavelet energy-based protection scheme for inverter-dominated microgrid,” IEEE Transactions on Smart Grid, vol. 13, no. 4, pp. 2533-2546, 2022.

[2] J. De La Cruz, Y. Wu, JE. Candelo-Becerra, JC. Vásquez, and JM. Guerrero, “A review of networked microgrid protection: Architectures, challenges, solutions, and future trends,” CSEE Journal of Power and Energy Systems., (future issue), pp. 1-25, 2023.

[3] B. John, A. Ghosh, M. Goyal, and F. Zare, “A DC power exchange highway based power flow management for interconnected microgrid clusters,” IEEE Systems Journal, vol. 13, no. 3, pp. 3347-3357, 2019.

[4] A. Barranco-Carlos, C. Orozco-Henao, J. Marín-Quintero, J. Mora-Flórez, and A. Herrera-Orozco, “Adaptive Protection for Active Distribution Networks: An Approach Based on Fuses and Relays With Multiple Setting Groups,” IEEE Access, vol. 11, pp. 31075-31091, 2023.

[5] F. Alsaeidi, CC. Liu, and LA. Lee, “Graph-theoretic partitioning for differential zone protection in an islanded microgrid,” In2023 IEEE Power & Energy Society Innovative Smart Grid Technologies Conference (ISGT), Washington, DC, USA, pp. 1-5, Jan 2023.

[6] B. Roy, S. Adhikari, S Datta, KJ. Devi, AD. Devi, F. Alsaif, S. Alsulamy, and TS Ustun, “Deep Learning based Relay for Online Fault detection, classification, and fault location in a grid-connected Microgrid,” IEEE Access, vol. 11, pp. 62674- 62696, 2023.

[7] A. Farshadi, BK. Eydi, H. Nafisi, H. Askarian-Abyaneh, and A. Beiranvand, “Rate of Change of Direct-Axis Current Component Protection Scheme for Inverter-Based Islanded Microgrids,” IEEE Access, vol. 11, pp. 46926-46937, 2023.

[8] X. Li, A. Dyśko, and GM. Burt, “Traveling wave-based protection scheme for inverter-dominated microgrid using mathematical morphology,” IEEE Transactions on Smart Grid, vol. 5, no. 5, pp. 2211-2218, 2014.

[9] D. Liu, A. Dyśko, Q. Hong, D. Tzelepis, and CD. Booth, “Transient wavelet energy-based protection scheme for inverter-dominated microgrid,” IEEE Transactions on Smart Grid, vol. 13, no.4, pp. 2533-2546, 2022.

[10] F. Zhang, and L. Mu, “New protection scheme for internal fault of multi-microgrid,” Protection and Control of Modern Power Systems, vol. 4, pp. 1-12, 2019.

[11] R. Escudero, J. Noel, J. Elizondo, J. Kirtley, “Microgrid fault detection based on wavelet transformation and Park’s vector approach,” Electric Power Systems Research, vol. 152, pp. 401-410, 2017.

[12] EB. Rocha Junior, OE. Batista, DS. Simonetti, “differential analysis of fault currents in a power distribution feeder using abc, αβ0, and dq0 reference frames,” Energies, vol. 15, no. 2, pp. 2-22, 2022.

[13] T. Kauffmann, U. Karaagac, I. Kocar, S. Jensen, J. Mahseredjian, and E. Farantatos, “An accurate type III wind turbine generator short circuit

model for protection applications," IEEE Transactions on Power Delivery, vol. 32, no. 6, pp. 2370-2379, 2016.

[14] S. Adhikari, F. Li, and H. Li, "PQ and PV control of photovoltaic generators in distribution systems," IEEE Transactions on Smart Grid, vol. 6, no.6, pp. 2929-2941, 2015